Mutation of Distal Residues of Horseradish Peroxidase: Influence on Substrate Binding and Cavity Properties†

Barry D. Howes,‡ Jose Neptuno Rodriguez-Lopez,§ Andrew T. Smith,|| and Giulietta Smulevich*,‡

Dipartimento di Chimica, Università di Firenze, Via G. Capponi 9, 50121 Firenze, Italy, Nitrogen Fixation Laboratory, John Innes Centre, Norwich, U.K., and Biochemistry Laboratory, University of Sussex, Brighton, U.K.

Received October 7, 1996; Revised Manuscript Received November 25, 1996⊗

ABSTRACT: The manner in which the distal heme pocket residues of peroxidases control the reaction mechanism and ligand binding has been investigated further by analysis of the electronic absorption and resonance Raman (RR) spectra of distal site mutants of recombinant horseradish peroxidase (HRP-C*). The roles of the conserved distal histidine and arginine residues, particularly in the context of the catalytic mechanism originally proposed for cytochrome *c* peroxidase (CCP), have been evaluated by studying the His42 → Leu, His42 → Arg, Arg38 → Gly, and Arg38 → Leu variants of HRP-C*. Spectra of the ferric forms, their complexes with benzohydroxamic acid (BHA), and the ferrous forms have been recorded at neutral pH. In addition, the ferric forms have been studied at alkaline pH. The relative populations of the three heme spin states characteristic of HRP-C* and its mutants were found to vary markedly from mutant to mutant. This diversity of heme spin state populations among the various mutants has allowed a well-defined set of RR frequencies to be compiled for the three heme spin states. These frequencies support the analysis of wild-type HRP-C* in terms of two heme states, five- (5cHS#) and six-coordinate high-spin (6cHS#), which exhibit anomalous RR frequencies compared to those of model heme systems. The third heme spin state is identified as being six-coordinate high-spin, displaying typical RR frequencies (6cHS). The 6cHS# and the 6cHS heme states are characterized by H bonding between the iron-bound water molecule and the Arg38 residue or the His42 residue, respectively. The proportion of six-coordinate high-spin heme states is at a minimum in the Arg38Leu mutant, indicating that the occupancy of the distal water molecule site is reduced in this mutant. The His42Arg mutant is distinguished from the other mutants by the unexpected presence of an iron-bound hydroxyl group at neutral pH. The spectral changes induced upon complexation with BHA indicate that both the distal histidine and arginine are involved in BHA binding; however, the arginine residue appears to play a more critical role. Measurements at pH 12 suggest there is a concerted involvement of both distal residues in mediating the alkaline transition of HRP-C*. Arg38 appears to be essential for stabilization of the OH^- ligand, while His42 acts as a H bond acceptor. A striking similarity between the roles of these residues in the reaction of H_2O_2 with the enzyme and the alkaline transition is noted. By comparison with the results from corresponding mutants of CCP, it appears that although the hydrogen-bonding network linking the distal and proximal sides of the heme is conserved the distal cavity in HRP-C differs significantly from that of CCP. However, some similarities in the local environment of the distal arginine are suggested.

Plant, fungal, and bacterial peroxidases have been divided into three groups on the basis of amino acid sequence alignment and structural divergences (Welinder, 1992). Class I, the intracellular peroxidases, includes cytochrome *c* peroxidase (CCP);[1] class II comprises the secretory fungal peroxidases such as *Coprinus cinereus* peroxidase (CIP), and class III contains the secretory plant peroxidases. A number of crystal structures of class I and class II enzymes have been reported, but until recently, the structure of a class III peroxidase was not available. The publication of the crystal structure of peanut peroxidase (PNP) (Schuller et al., 1996), the first example of a class III peroxidase structure, will without doubt provide the basis for more focused studies of class III peroxidases. In particular, it promises to serve as a good model for horseradish peroxidase (HRP-C), also a class III peroxidase and one of the most extensively studied peroxidases (Dunford & Stillman, 1976; Dunford, 1991). Indeed, it is evident from the crystal structure that PNP has

† The work was supported by grants from the Italian Consiglio Nazionale delle Ricerche (CNR) and Ministero della Università e Ricerca Scientifica e Tecnologica (MURST) (to G.S.) and the EC Human Capital and Mobility Programme (to A.T.S. and G.S.) (ERB CHRX-CT92-0012-130). B.D.H. and J.N.R.-L. are funded by fellowships from the EC as part of the above program.

* Author to whom correspondence should be addressed. E-mail: Smulev@chim.unifi.it.

‡ Università di Firenze.

§ John Innes Centre.

|| University of Sussex.

⊗ Abstract published in *Advance ACS Abstracts,* January 15, 1997.

[1] Abbreviations: CCP, cytochrome *c* peroxidase; CIP, *Coprinus cinereus* peroxidase; PNP, peanut peroxidase; HRP-C*, recombinant horseradish peroxidase isoenzyme C; F41V, Phe41 → Val HRP-C* mutant; F41W, Phe41 → Trp HRP-C* mutant; R38K, Arg38 → Lys HRP-C* mutant; R38G, Arg38 → Gly HRP-C* mutant; R38L, Arg38 → Leu HRP-C* mutant; H42L, His42 → Leu HRP-C* mutant; H42R, His42 → Arg HRP-C* mutant; metMb, metmyoglobin; RR, resonance Raman; NMR, nuclear magnetic resonance; ABTS, 2,2′-azinobis(3-ethylbenzothiazolinesulfonic acid); BHA, benzohydroxamic acid; MOPS, 3-morpholinopropanesulfonic acid; 5c and 6c, five-coordinate and six-coordinate hemes, respectively; HS and LS, high- and low-spin, respectively; CT1, long wavelength (>600 nm) porphyrin-to-metal charge transfer band.

S0006-2960(96)02502-0 CCC: $14.00

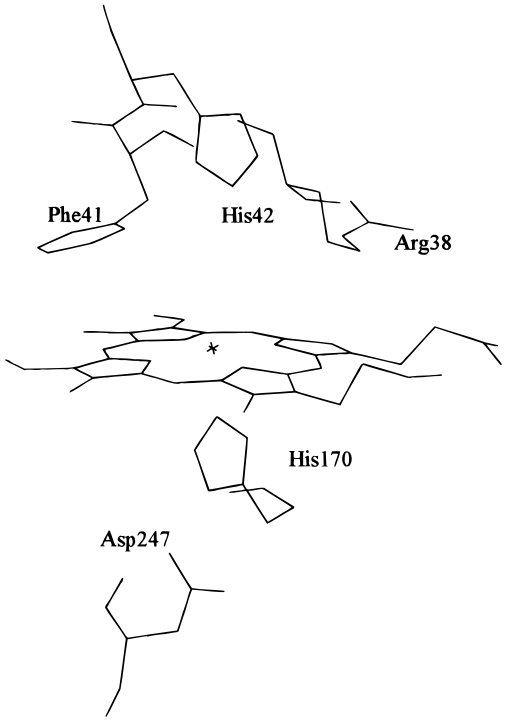

FIGURE 1: Model of the disposition of the amino acid residues in the heme pocket of HRP-C based on the X-ray crystal structure of CCP (Finzel et al., 1984) and modeling studies (Smith et al., 1994).

a smaller heme core size compared to CCP and vinyl torsion angles which are different from each other and, moreover, significantly different from those of CCP.

The plant peroxidase superfamily has a number of conserved residues on both the distal and proximal sides of the heme (Welinder, 1992). These residues, *viz.* the distal histidine and arginine and the proximal histidine and aspartate, have been proposed to play key roles in the catalytic mechanism. A model illustrating the disposition of the heme pocket residues of HRP-C is shown in Figure 1. A concerted program of kinetic and spectroscopic techniques applied to wild-type and mutant forms of HRP-C and other peroxidases, in particular CCP, has provided the foundation from which it is now possible to have an initial understanding of the influence of the protein environment of the heme on the catalytic mechanism. Resonance Raman (RR) spectroscopy has played an important part in providing information on the heme pocket of HRP-C (Rakshit & Spiro, 1974; Teraoka & Kitagawa, 1981; Evangelista-Kirkup et al., 1985; Smulevich et al., 1994b) and CCP (Sievers et al., 1979; Hashimoto et al., 1986; Dasgupta et al., 1989; Smulevich et al., 1988a,b, 1989a,b, 1990a,b, 1991b; Smulevich, 1993). Comparative studies of these two proteins have suggested that the heme pocket structure is significantly different, whereas the hydrogen-bonding network extending between the distal and proximal sides of the heme is maintained (Smulevich et al., 1994b).

The heme pocket of the recombinant wild-type enzyme (HRP-C*) had been found by RR (Smulevich et al., 1994b), electronic absorption (Smith et al., 1992), and ^{1}H NMR data (Veitch et al., 1992) to be identical to that of the commercially available plant enzyme (HRP-C). RR spectroscopy has also shown that HRP-C exists as a mixture of 6cHS and 5cHS forms (Terner & Reed, 1984; Smulevich et al., 1991a), the latter being the dominant form. Subsequent work by Smulevich et al. (1994b) showed that the frequencies of the ν_3 and ν_{10} core size marker bands in HRP-C are about 10 cm^{-1} higher than those normally observed for 5cHS and 6cHS hemes in model compounds. To distinguish them from "normal" hemes, they were referred to as 5cHS$^{\#}$ and 6cHS$^{\#}$, respectively. This is the first example of a hemoprotein displaying such effects, and it is suggested to be a consequence of the high-spin heme in HRP-C* having a different degree of distortion from planarity and/or a more contracted core compared to that of other heme proteins. Disruption of the distal structure by mutation or aromatic donor binding partially relieves this effect, resulting in a new species characterized by core size marker band frequencies corresponding to those of 6cHS model compound hemes.

In the present study, electronic absorption and RR data from the recombinant HRP-C (HRP-C*) distal site mutants His42 → Leu (H42L), His42 → Arg (H42R), Arg38 → Leu (R38L), and Arg38 → Gly (R38G) are presented and compared with those of other distal site mutants of HRP-C* and with those of the corresponding mutants of CCP. This has highlighted both similarities and differences in the detailed heme pocket structure of the two proteins. Mutation of the two key distal pocket residues (His42 and Arg38) has, furthermore, provided insight into the coupled nature of their roles in the binding of benzohydroxamic acid (BHA) and hydrogen peroxide to HRP-C*.

EXPERIMENTAL PROCEDURES

Sample Preparation. Production and expression procedures for the mutants in recombinant HRP-C* have been described elsewhere (Smith et al., 1992; Meunier et al., 1995). Purified enzyme (in 10 mM MOPS at pH 7) with a concentration of about 10−30 μM was used for Raman excitation in the Soret band and about 100 μM for excitation in the visible region. The RZ (Reinheitszahl) values and specific activities (units per milligram) of the preparations used in this work were as follows: H42L, 3.4 and 0.3; H42R, 3.2 and 5.0; R38L, 3.2 and 5.2; and R38G, 3.4 and 47.7, respectively. The activity was measured with 0.3 mM ABTS and 2.5 mM H_2O_2 (Smith et al., 1990). The ferrous samples were prepared by adding 2 μL of dithionite (20 mg mL^{-1}) to 50 μL of deoxygenated peroxidase solution.

The aromatic donor complexes with benzohydroxamic acid (BHA, Sigma) were made by adding 0.2 M BHA to give the required final concentration, corresponding to *ca*. 90% saturation of the BHA complex formation. The BHA concentration used for the RR sample of the R38L mutant corresponded to *ca.* 70% saturation, although measurements made for 90% saturation showed negligible changes in the RR spectrum. The spectra of all mutants displayed minimal differences for BHA saturation greater than 90%, but an intense RR BHA band at 1604 cm^{-1} is evident. The dissociation constants (millimolar), K_d, for BHA binding to the mutants are as follows: H42L, 2.9; H42R, 6.8; R38L, >12.1; and R38G, 10.4.

The hydroxide complexes were prepared by adding small amounts of de-aerated NaOH (*ca*. pH 13) to de-aerated protein solutions followed by rapid stirring, until the desired pH was obtained. De-aerated samples were used to avoid formation of carbonic acid and consequent lowering of the pH. The OD$^-$ complexes were prepared by lyophilization of samples at pH 7. The lyophilized material was redissolved

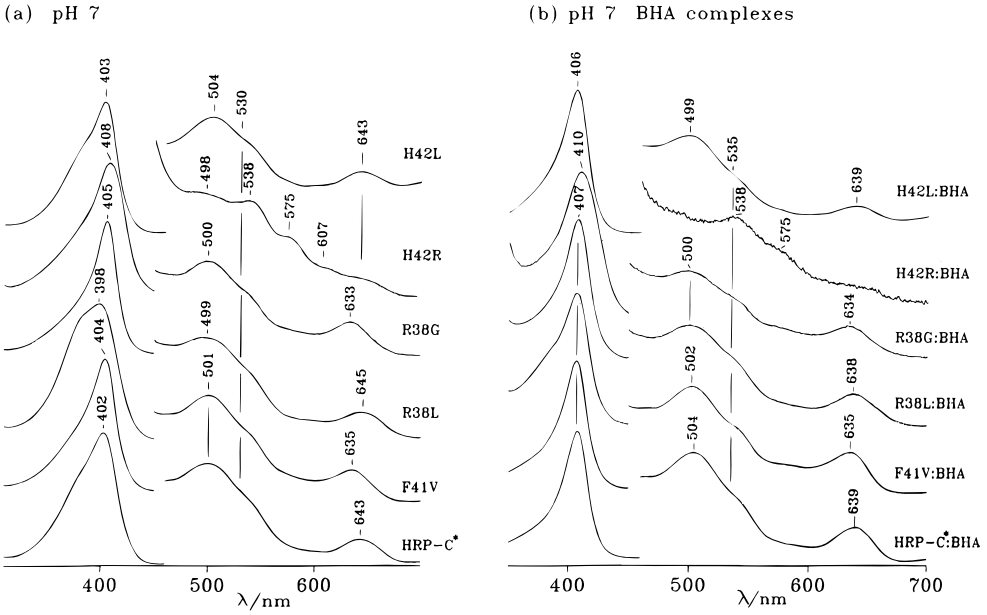

FIGURE 2: Absorption spectra of recombinant HRP-C* and the distal mutants F41V, R38L, R38G, H42R, and H42L at pH 7 (a) and of their BHA complexes at pH 7 (b).

Table 1: Absorption Maxima (nm) and Heme Spin Forms Present in Wild-Type HRP-C*, Mutants, and Their BHA Complexes[a]

						BHA complexes				
			spin states					spin states		
	Soret	CT1	5cHS[#b]	6cHS[#b]	6cHS	Soret	CT1	5cHS[#b]	6cHS[#b]	6cHS
R38L	398	645	s	vw		407	638	m	m	m
HRP-C*	402	643	s	w		407	639		s	m
H42L	403	643	vw	s	vw	406	639		w	s
F41V	404	635	w	w	m	407	635		w	m
R38G	405	633	vw	w	m	407	634	vw	w	m

[a] 5c and 6c, five-coordinate and six-coordinate, respectively; HS, high-spin; LS, low-spin; vw, w, m, and s, very weak, weak, medium, and strong (relative intensities of RR bands roughly correspond to the species abundance). [b] Heme species showing core size marker bands with atypical frequencies compared to corresponding heme model compounds.

in D_2O and the pH adjusted to the final value using NaOD, following the procedure outlined for the hydroxide complex. The RR spectra of the lyophilized samples at pH 7 were identical to those obtained for nonlyophilized samples, indicating that the proteins are not damaged by lyophilization. The fluoride samples were prepared by adding NaF crystals to solutions of the mutants at pH 5.

Electronic Absorption and RR Spectroscopy. The RR spectra were obtained at room temperature with excitation from the 406.7, 413.1, and 530.9 nm lines of a Kr^+ laser (Coherent, Innova 90/K) and from the 457.9 and 496.5 nm lines of an Ar^+ laser (Coherent, Innova 90/5). The back-scattered light from a slowly rotating NMR tube was collected and focused into a computer-controlled double monochromator (Jobin-Yvon HG2S) equipped with a cooled photomultiplier (RCA C31034A) and photon counting electronics. To minimize local heating of the protein by the laser beam, the sample was cooled by a gentle flow of N_2 gas passed through liquid N_2. To maintain sample integrity for a minimum of 1 h, cooling was found to be necessary for the H42R, R38G, and R38L variants.

The RR spectra were calibrated to an accuracy of 1 cm^{-1} for intense isolated bands, with indene as the standard for the high-frequency region and with indene and CCl_4 for the low-frequency region. Polarized spectra were obtained by inserting a polaroid analyzer between the sample and entrance slit of the monochromator. The depolarization ratios of the bands at 314 and 460 cm^{-1} of CCl_4 were measured to check the reliability of the polarization measurements. The values obtained, 0.73 and 0.00, compared well with the theoretical values of 0.75 and 0.00, respectively. To determine peak intensities, a curve-fitting program was used to simulate experimental spectra using Lorentzian line shapes.

The absorption spectra were measured with a Cary 5 spectrophotometer.

RESULTS

Characterization of the Mutants

Electronic Absorption Spectroscopy. Figure 2a presents the electronic absorption spectra of wild-type HRP-C* and a number of distal site mutants (H42L, H42R, R38G, R38L, and F41V) at pH 7. Spectra of the wild-type enzyme and its F41V variant have been reported previously (Smith et al., 1992). The positions of the absorption maxima and the heme spin states found to be present (from both absorption and RR spectra) for each mutant have been collected in Table 1 to aid comparison of the properties of the various mutants. Significant differences are observed between wild-type HRP-C* and its mutants, particularly in the position of the Soret and CT1 bands. The wild-type spectrum is consistent with a 5cHS heme and has also been characterized by RR spectroscopy to have a dominant 5cHS heme species (Smulevich et al., 1994b). The red shift and narrowing of

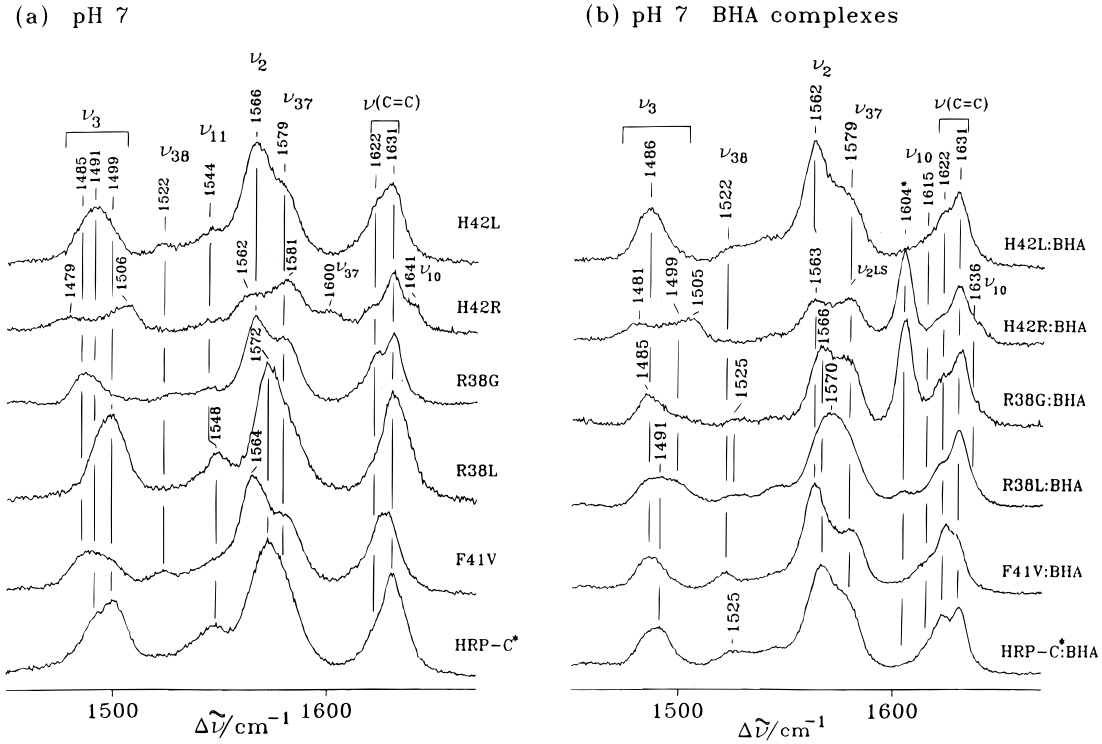

FIGURE 3: (a) Resonance Raman spectra of recombinant HRP-C* and the distal mutants F41V, R38L, R38G, H42R, and H42L at pH 7, recorded with 406.7 nm excitation. Experimental conditions were as follows: 5 cm^{-1} resolution; 6 s per 0.5 cm^{-1} collection interval, 30 mW laser power at the sample (HRP-C*, F41V, R38L, and H42L); 15 s per 0.5 cm^{-1} (R38L) and 8 s per 0.5 cm^{-1} (H42R) collection interval, 15 mW laser power at the sample. (b) Resonance Raman spectra of the BHA-complexed forms of recombinant HRP-C* and the distal mutants F41V, R38L, R38G, H42R, and H42L at pH 7 with excitation at 406.7 nm. Experimental conditions were as follows: 5 cm^{-1} resolution, 4 s per 0.5 cm^{-1} (HRP-C*, F41V, and H42L) and 9 s per 0.5 cm^{-1} (R38L, R38G, and H42R) collection interval, 30 mW laser power at the sample. The * indicates a band due to BHA.

the Soret band with respect to that of the wild type for all the mutants except R38L indicate that these have a higher proportion of 6cHS heme. A blue shift of the CT1 band is also normally expected to be associated with a higher proportion of 6cHS. It is evident from Figure 2a, however, that only the F41V and R38G mutants exhibit a clear blue shift of the CT1 band. The influence of hydrogen bonding on the position of the CT1 band is assessed in the Discussion. The blue shift of the Soret band and the red shift of the CT1 band for R38L are suggestive of a higher proportion of 5cHS heme in this variant than in HRP-C*. The H42R mutant can be distinguished from all the other HRP-C* variants that have been studied at neutral pH. In fact, the visible region of the spectrum, with bands at 538, 575, and 607 nm, is more reminiscent of that normally observed at alkaline pH for heme proteins (Feis et al., 1994). The broad Soret and the bands at 643 and 498 nm, however, indicate that a small proportion of the heme spin forms found in wild-type HRP-C* remains.

Resonance Raman Spectroscopy. The high-frequency regions of the RR spectra of the four mutants under investigation are shown in Figure 3a for Soret excitation, and for comparison, the corresponding spectra of HRP-C* and its F41V mutant (Smulevich et al., 1994b) are also included. The three distal site mutants of HRP-C* previously studied by RR spectroscopy, *viz.* Arg38 → Lys (R38K), Phe41 → Val (F41V), and Phe41 → Trp (F41W), all exhibited an extra peak at about 1486 cm^{-1} (in addition to those corresponding to 5cHS[#] and 6cHS[#]) on the low-frequency side of the ν_3 band corresponding to a normal 6cHS (Smulevich et al., 1994b). Simulations of the ν_3 region of the RR spectra of H42L and R38G (data not shown) indicate that these mutants are also a mixture of three spin states. The band is composed of peaks at 1491 and 1499 cm^{-1} corresponding to 6cHS[#] and 5cHS[#] forms, respectively, with anomalous frequencies, as previously identified for HRP (Smulevich et al., 1994b). In addition, there is a peak at 1485 cm^{-1} due to a 6cHS form, with associated peaks evident for other core size marker bands (Table 2). However, it is clear from the different spectral line shapes that the relative populations of the heme spin states are different in the two mutants. The 6cHS[#] form is dominant in H42L, whereas the 6cHS form is dominant in R38G together with a much

Table 2: Resonance Raman Frequencies (cm^{-1}) of the Heme Spin Forms Present in Wild-Type HRP-C* and Mutants[a]

				model compounds[b]	
mode	6cHS	6cHS[#c]	5cHS[#c]	6cHS	5cHS
ν_3	1485	1491	1499	1480	1491
ν_{38}	1521	1522		1518	1533
ν_{11}	1544	1545	1549	1545	1553
ν_2	1562	1566	1572	1559	1570
ν_{19}	1561	1569	1572	1560	1571
ν_{37}	1579			1580	1591
ν(C═C)		1622			
ν(C═C)		1631			
ν_{10}	1615	1621	1636	1610	1626

[a] 5cHS and 6cHS, five-coordinate high-spin and six-cHS high-spin, respectively. [b] RR frequencies of model heme compounds (Choi et al., 1982). [c] Hemes that differ in the frequencies of some core size marker bands with respect to model compounds. Frequencies were determined from the experimentally observed band positions of various mutants as described in the text, using essentially the H42L−BHA complex for 6cHS, H42L for 6cHS[#], and R38L for 5cHS[#].

reduced contribution from the 5cHS# heme compared with HRP-C* and the other mutants.

The spectrum of R38L is very similar to that of HRP-C*. Closer inspection and simulation of the ν_3 band (data not shown) demonstrate that, although R38L is a mixture of 5- and 6cHS# hemes, it has an increased proportion of 5cHS# (1499 cm^{-1}) compared to HRP-C*, in agreement with the result noted for the absorption spectrum. It is of interest that this is the first distal mutation of HRP-C* which does not give rise to a 6cHS heme species. Both of these observations clearly indicate that the occupancy of the distal water molecule site is reduced in this mutant. The crystal structure of the corresponding CCP mutant (R48L) demonstrates a similar low occupancy of the water molecule site, consistent with the observed pentacoordinate state of the heme (Smulevich et al., 1988a; Vitello et al., 1993).

The H42R variant is characterized by a RR spectrum that is quite different from all the other HRP-C* distal mutants studied so far. The ν_3 mode displays two distinct bands at 1479 and 1506 cm^{-1}, which are assigned to 6cHS and 6cLS hemes, respectively (Choi et al., 1982). The 6cHS band is placed at a lower frequency (1479 cm^{-1}) than that observed for the other mutants (1485 cm^{-1}), suggesting that it results from a different ligand bond to the iron atom than that at 1485 cm^{-1}. Bands in the ν_2 region at 1562 and 1581 cm^{-1} are assigned to 6cHS and 6cLS hemes, respectively. Finally, bands at 1600 and 1641 cm^{-1} are assigned to LS heme forms of the ν_{37} and ν_{10} modes, respectively. The broadness of all the bands suggests that, in addition to the two dominant heme spin forms characterized by the above RR frequencies, there is also present a small proportion of the three heme spin states found in the other mutants. The general spectral shape is strangely highly reminiscent of that seen for heme proteins at alkaline pH (Feis et al., 1994), as previously noted from its absorption spectrum.

The strong resemblance of the absorption and RR spectra of the H42R mutant at pH 7 (Figures 2a and 3a) to those observed for hemoproteins at alkaline pH (Feis et al., 1994) prompted an H/D exchange study. Figure 4 shows the low-frequency RR spectra of H42R in H_2O and D_2O at pH 7. Identical spectra were obtained at pH 12. The most marked effect of the H/D exchange is the detection of an isotope-sensitive band found at 490 cm^{-1} in the D_2O sample and placed at 501 cm^{-1} in the H_2O sample by calculating the expected shift on deuterium exchange using the biatomic oscillator Fe−OH model. This band is assigned as the high-spin Fe−OH stretching frequency by comparison with methemoglobin (see Effect of Alkaline pH).

The vinyl stretching mode frequencies given in Table 2 have been identified, by Soret excitation (406.7 nm), as polarized bands at 1622 and 1631 cm^{-1}. It was found that the vinyl modes are still enhanced with visible excitation, with bands which overlap those of the ν_{10} mode. The vinyl modes are not expected to be enhanced upon visible excitation as they are totally symmetric modes; however, the same effect has been observed for CCP (Smulevich et al., 1990), CIP (Smulevich et al., 1994a), and HRP-C* (Smulevich et al., 1994b).

A comparison of the spectra in Figure 3a, particularly the ν_3 band (see also Table 1), reveals significant differences in the relative populations of the three heme spin forms characteristic of HRP-C* and its distal mutants. These variations range from the R38L variant which exhibits the maximum population of 5cHS# and no 6cHS heme, to the H42L mutant which displays all three forms and has a dominant 6cHS# heme, to the R38G variant which shows the maximum population of 6cHS and very little 5cHS# heme. It is noted that the anomalous 5- and 6cHS# hemes of HRP-C* may have Franck−Condon factors (A_{1g} modes) and vibronic coupling terms (B_{1g} and A_{2g} modes) different from those observed for normal hemes. Therefore, any discussion of absolute percentages of heme species should be approached with caution. However, comparison of mutants to determine differences in relative populations is unaffected by these effects. By the appropriate choice of mutant, these considerable differences in the relative populations of the heme spin states were exploited, together with the RR measurements in the presence of saturating BHA (see below), to compile Table 2. The RR frequencies shown for a given heme spin state are those displayed by a mutant which has this particular heme species as its dominant spin state. The spectra of the R38L and H42L mutants are used to generate the 5- and 6cHS# columns, respectively, of Table 2. The 6cHS column is determined from the H42L−BHA complex. The RR frequencies reported in Table 2 have been determined from the high-frequency region of the RR spectra with excitation in the Soret band and, for HRP-C*, R38L and H42L, also in the visible region, wild-type HRP-C* and R38L at 530.9 nm and H42L at 496.5 nm. Assignment of the various bands to particular vibrational modes has been

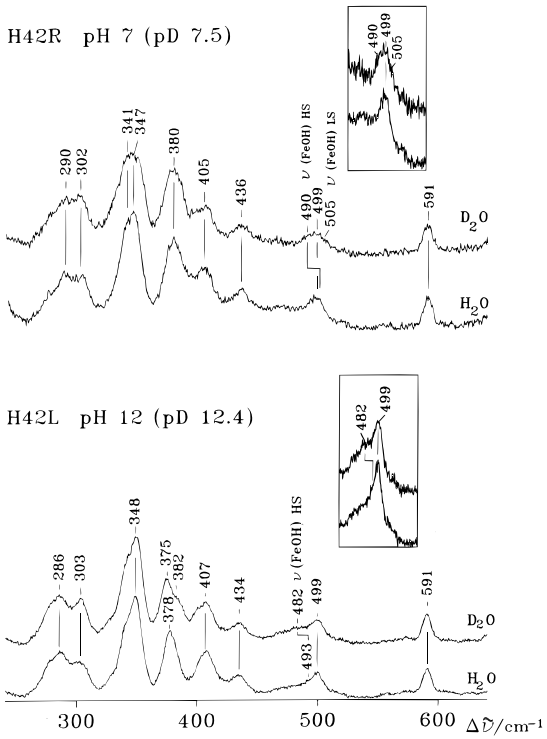

FIGURE 4: (Top) Resonance Raman spectra of the H42R mutant at pH 7 (pD 7.5) with excitation at 413.1 nm in H_2O and D_2O. Experimental conditions as follows: 5 cm^{-1} resolution, 19 s per 0.5 cm^{-1} (H_2O) and 12 s per 0.5 cm^{-1} (D_2O) collection interval, 15 mW laser power at the sample. Identical spectra were obtained at pH 12 (pD 12.5). (Bottom) Resonance Raman spectra of the H42L mutant at pH 12 (pD 12.4) with excitation at 413.1 nm in H_2O and D_2O. Experimental conditions were as follows: 5 cm^{-1} resolution, 16 s per 0.5 cm^{-1} collection interval, 15 mW laser power at the sample. The insets show an expansion of the ν(Fe−OH) stretching region in the frequency range of 450−550 cm^{-1}. HS and LS indicate bands due to high-spin and low-spin hemes, respectively.

confirmed by recording spectra in polarized light and using a curve-fitting program to determine band intensities.

The trend of an increasingly red-shifted Soret band and blue-shifted CT1 band (Figure 2a and Table 1) with respect to those of R38L in the order HRP-C*, H42L, F41V, and R38G is reflected in the RR spectra (Figure 3a) by an increasing population of 6cHS in the same order.

Effect of BHA

Figure 2b shows the absorption spectra of the BHA complexes, for at least 90% BHA saturation, of HRP-C* and the five distal mutants under consideration. It is evident from Table 1 and comparison of panels a and b of Figure 2 that the Soret bands of all the BHA complexes are red-shifted by a minimum of 2 nm (H42R and R38G) to a maximum of 9 nm (R38L), clearly indicative of a progressive increase in the population of the 6cHS heme state. The CT1 bands of the BHA complexes of HRP-C*, H42L, and R38L are blue-shifted, consistent with an increased proportion of 6cHS heme, whereas that of F41V and R38G, for which the 6cHS state was already abundant in the absence of BHA, remains at 635 nm and is red-shifted by only 1 nm, respectively.

The RR spectra, with Soret excitation, of the BHA complexes are presented in Figure 3b. The amount of BHA added was sufficient to give at least 90% saturation, except for the R38L complex which was 70% saturated. However, no further changes were seen in the spectra up to 90% saturation. Therefore, to avoid the intense BHA band at 1604 cm^{-1}, the 70%-saturated spectrum is shown. The spectra of HRP-C*−BHA and the variant F41V−BHA have been published previously (Smulevich et al., 1994b). A comparison of the spectra with those of Figure 3a shows that BHA has a considerable effect on some of the mutants, indicating that the relative populations of the spin forms are modified by BHA (see also Table 1). Smulevich et al. (1994b) have shown that for HRP-C*−BHA and F41V−BHA these changes correspond to an increase in the population of the 6cHS form at the expense of the 5cHS$^{\#}$ form, which completely disappears. In HRP-C*−BHA, the 6cHS$^{\#}$ heme form dominates, whereas in F41V−BHA, it is the 6cHS form. Simulations (data not shown) and visual inspection of the ν_3 bands of the other mutants shown in Figure 3b indicate that the 6cHS form is also dominant in H42L−BHA and that no 5cHS$^{\#}$ heme remains. However, even if the line shape of the ν_3 bands of the F41V−BHA and H42L−BHA complexes appears similar, differences in other parts of the RR spectrum, particularly the broader bands in the ν_{38} and ν_2/ν_{37} regions and the different relative intensity of bands in the ν_{10}/vinyl region, suggest that this may not be the case and that the 6cHS$^{\#}$ population is slightly higher than the 6cHS population in H42L−BHA. Nevertheless, an interpretation based on a dominant 6cHS heme is favored by the observed equivalence of the RR frequencies of H42L−BHA and F41V−BHA. The R38L mutant, which alone displayed a clearly dominant 5cHS$^{\#}$ heme and no 6cHS heme, in the presence of BHA is a mixture of 6cHS, 6cHS$^{\#}$, and 5cHS$^{\#}$ hemes in roughly equal proportions. The complexes of the R38G and H42R variants show a minor increase in the population of the 6cHS heme but retain some 5cHS$^{\#}$ heme and are largely unchanged with respect to their spectra in the absence of BHA. The shoulders at 1499 and 1636 cm^{-1} in the BHA complexes of the H42R, R38G, and R38L

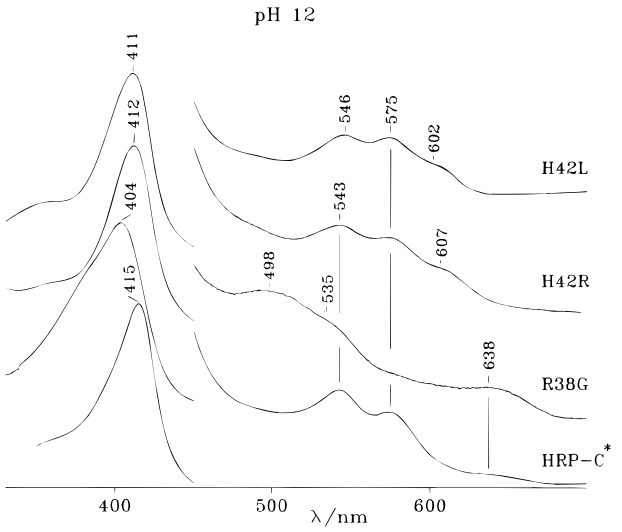

FIGURE 5: Absorption spectra of recombinant HRP-C* and the distal mutants R38G, H42R, and H42L at pH 12.

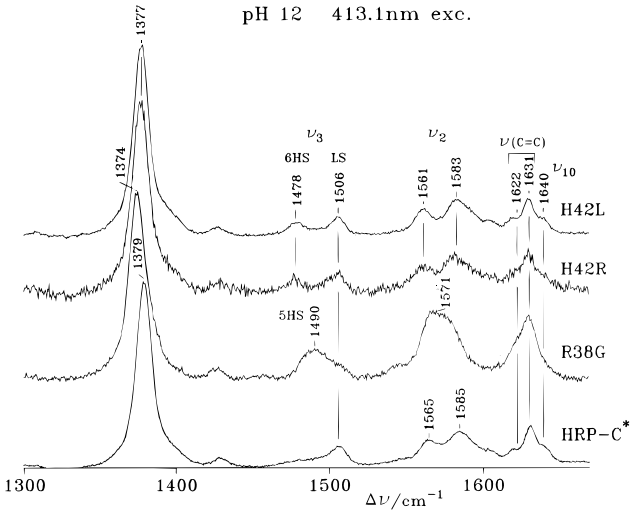

FIGURE 6: Resonance Raman spectra of recombinant HRP-C* and the distal mutants R38G, H42R, and H42L at pH 12 with excitation at 413.1 nm. Experimental conditions were as follows: 5 cm^{-1} resolution, 5 s per 0.5 cm^{-1} (HRP-C*, H42R, and H42L) and 12 s per 0.5 cm^{-1} (R38G) collection interval, 15 mW laser power at the sample. 5HS and 6HS indicate that the bands are due to 5- and 6cHS hemes, respectively, and LS indicates that the band results from the low-spin heme.

mutants are assigned to the ν_3 and ν_{10} modes, respectively, of the small amount of 5cHS$^{\#}$ heme which remains in these complexes. In addition, for the H42R mutant, bands due to the 6cLS heme are still present at 1505 and 1579 cm^{-1} and bands due to the 6cHS heme at 1481 and 1563 cm^{-1}. The 6cHS and 5cHS$^{\#}$ ν_{10} bands at 1615 cm^{-1} (HRP-C*−BHA, F41V−BHA, R38L−BHA, and H42L−BHA) and 1636 cm^{-1} (H42R−BHA, R38G−BHA, and R38L−BHA), respectively, were also evident in the polarized RR spectra without BHA for Soret excitation (data not shown). The intensification and depolarized nature of these bands observed upon visible excitation allowed them to be clearly assigned to ν_{10} modes.

Effect of Alkaline pH

Figures 5 and 6 present absorption and RR spectra, respectively, of the H42L, H42R, and R38G variants at pH 12. The spectra of HRP-C* (Feis et al., 1994) are also shown

for comparison. The absorption spectra of H42L and H42R display a shoulder at 602 and 607 nm, respectively, which is assigned to a charge transfer band of a high-spin heme by analogy with that observed for metmyoglobin (metMb) (Asher & Schuster, 1979). In fact, it is absent in the wild-type protein which has only a few percent of high-spin heme (George et al., 1964). In addition, an essentially identical spectrum has been obtained for methemoglobin at alkaline pH (Feis et al., 1994), which is known to be a 55:45 mixture of low- and high-spin hemes. It is of interest to note that all the bands present in the visible region of the H42R spectrum at pH 12 are already evident at pH 7 (Figure 2a).

The ν_3 bands of the RR spectra of the H42L and H42R mutants are clearly split into two components at frequencies which correspond to 6cHS (1478 cm^{-1}) and 6cLS (1506 cm^{-1}) hemes, contrasting with HRP-C* which shows only a 6cLS band. These results are further confirmed by the low-frequency region RR spectra of H42R and H42L at pH 12 in H_2O and D_2O (Figure 4). The isotope-sensitive band found in the D_2O sample of H42L at 482 cm^{-1} is placed at 493 cm^{-1} in the H_2O sample by calculating the expected shift on deuterium exchange using the biatomic oscillator Fe−OH model. This band is assigned as the high-spin ν(Fe−OH) stretching frequency by analogy with the 495 cm^{-1} band of methemoglobin, identified as high-spin by excitation at 600 nm (Asher & Schuster, 1979). The low-spin ν(Fe−OH) stretching mode is expected at 503 cm^{-1} and should undergo an upshift of about 6 cm^{-1} on deuterium exchange, by analogy with the behavior of wild-type protein (Sitter et al., 1988). This band is weak and hidden under the porphyrin band at 499 cm^{-1} and, hence, difficult to observe.

The low-frequency RR spectra of H42R at pH 12 in H_2O and D_2O are identical to those observed at pH 7 (Figure 4). This is consistent with the strong similarity of the visible absorption spectra at pH 7 and 12 (Figures 2a and 5) which, furthermore, is also the case for the high-frequency RR spectra (Figures 3a and 6). Following the same argument outlined above for the H42L mutant, the isotope-sensitive band found in the D_2O sample of H42R at 490 cm^{-1} is placed at 501 cm^{-1} in the H_2O sample and assigned as the high-spin ν(Fe−OH) stretching frequency. The high-spin ν(Fe−OH) stretching frequency is significantly shifted (by 8 cm^{-1}) to higher frequency in the H42R variant compared to that in H42L, indicating a stronger Fe−OH bond in H42R. Contrary to the case of H42L, it has been possible to identify the low-spin ν(Fe−OD) stretching mode in the D_2O spectrum of H42R (Figure 4), at a slightly lower frequency (505 cm^{-1}) than that expected by analogy with HRP-C*.

The R38G mutant, which at neutral pH was found by both absorption and RR spectroscopy to have an essentially 6cHS heme, at alkaline pH is predominantly characteristic of a 5cHS heme. This is inferred by the blue shift of the Soret and the red shift of the charge transfer band at alkaline pH (Figure 5) and by RR frequencies (Figure 6) typical of 5cHS hemes (Choi et al., 1982). A small amount of low-spin heme is also suggested by the weak absorption bands at 543 and 575 nm and RR bands assigned as low-spin ν_3 and ν_{10} modes at 1506 and 1640 cm^{-1}, respectively.

The absorption spectrum of the R38L mutant at pH 12 (data not shown) is identical to that at pH 7, indicating that the Arg residue is essential for the Fe−OH bond to form.

Table 3: ν(Fe−Im) Stretching Frequencies (cm^{-1}) of Distal Mutants of CCP and HRP at pH 7.0

mutation	CCP	HRP
wild type	233, 246[a]	243[c]
Arg → Leu	242[a]	238[d]
Arg → Lys	233, 246[a]	240[c]
Arg → Gly		241[d]
His → Leu	241[b]	238[d]
His → Arg		242[d]
Phe → Val		242[c]

[a] Smulevich et al. (1988). [b] Smulevich et al. (1991). [c] Smulevich et al. (1994). [d] Present work.

This is consistent with the results obtained for the R38G and R38K (Sanders et al., 1994) mutants.

Ferrous Hemes

At neutral pH, the reduced form of the H42L, H42R, R38G, and R38L mutants is characterized by a 5cHS heme (data not shown), consistent with wild-type HRP-C* and the other distal variants previously studied (Smulevich et al., 1994b). A strong band at 243 cm^{-1} in the ferrous form of the wild-type enzyme has been assigned to the stretching mode of the bond between the iron and the proximal imidazole side chain of His170 (Teraoka & Kitagawa, 1981). Table 3 shows the ν(Fe−Im) stretching frequencies of HRP-C* and CCP distal mutants. It is evident that only the H42L, R38G, R38L, and R38K mutations (HRP numbers) cause a change (downshift) in the frequency. The effect on Arg → Lys mutation is seen, however, only for HRP-C. The H42R and F41V mutations have only a slight effect (1 cm^{-1} downshift) on the ν(Fe−Im) stretching frequency.

DISCUSSION

Ferric Hemes. Previous work on CCP (Smulevich et al., 1991b) has shown that mutation of the distal His residue, *viz*. His52Leu, induces only very minor changes in the RR spectra at neutral pH, resulting from an increased proportion of 5cHS heme. The present study has demonstrated that considerable changes are induced by mutation of the distal histidine in HRP-C*, reflecting significant increases in 6cHS forms of the heme at the expense of the $5cHS^{\#}$ heme. However, mutations of the distal arginine in CCP, *viz*. Arg48 → Lys and Leu (Smulevich et al., 1988a; Vitello et al., 1993), give rise to changes which have some similarities with those observed for corresponding variants of HRP-C*. The RR spectra of the Arg → Lys mutant for both proteins show some 6cLS heme, suggesting partial binding of the lysine. The crystal structure, however, of the CCP mutant apparently indicates that the Lys48 side chain does not coordinate to the heme iron, although it does move toward the heme iron, displacing distal water molecule 595. The crystal structure of the CCP R48L mutant shows that substitution of Arg48 by leucine causes a considerable decrease in the level of occupancy of the water 595 site and the iron atom moves 0.2 Å toward the proximal side of the heme. These observations are in agreement with the RR data of this mutant which indicate a 5cHS heme only, at neutral and lower pH (Smulevich et al., 1988a). The HRP R38L variant exhibits similar behavior, having an increased proportion of $5cHS^{\#}$ heme with respect to wild type. It follows from the above discussion that corresponding mutants of the distal arginine

in CCP and HRP-C* display similar trends, whereas this is not the case for the distal histidine mutants. It is therefore evident that the distal heme pocket structures are different in the two proteins; however, the position and local structure around the distal arginine in the two proteins must have some common characteristics.

The compilation of Table 2, by appropriate choice of mutants which display one of the three characteristic heme forms as their dominant species, and the reproducibility of the RR frequencies (*e.g.* H42L−BHA and F41V−BHA display the same RR frequencies), has enabled all the RR frequencies of the three heme forms to be clearly defined. This permits previous observations of anomalously high frequencies for some RR modes of HRP-C* (Smulevich et al., 1994b) to be confirmed. Only C_a-C_m bridge bond stretching modes appear to be affected. The ν_3 and ν_{10} modes for both the 5cHS$^{\#}$ and 6cHS$^{\#}$ hemes and the ν_{19} mode for only the 6cHS$^{\#}$ heme form displayed RR frequencies about 10 cm^{-1} higher than those found in model compounds. The sensitivity of these modes to the out-of-plane displacement of the C_m atoms and, consequently, deformation of the heme may be an important factor in determining this behavior (Smulevich et al., 1994b).

The sensitivity of the CT1 band wavelength to the nature of the proximal and distal ligands of the heme iron and, in particular, to hydrogen bonding effects has recently been amply demonstrated (Smulevich et al., 1996, 1997). Such effects have been alluded to previously in the literature (Asher et al., 1981). Information on the hydrogen bonding status of the axial ligands is clearly of considerable importance in the study of the function of the protein. Smulevich and co-workers show that if the ligand acts as a H bond donor then the stronger the hydrogen bond, the lower the wavelength of the CT1 band. If the ligand acts as a H bond acceptor, the CT1 band wavelength increases with the strength of the H bond. Therefore, if one considers the proximal ligand to remain unchanged, a comparative study of the nature and strength of H bonding to the sixth ligand of a number of heme proteins is possible. In the context of studies on peroxidases, the sixth ligand is very often a water molecule. An indication of the approximate CT1 wavelengths corresponding to the H bonded (to the distal histidine residue) and nonbonded states of the distal water molecule can be obtained by analogy with the case of ferric metMb. At neutral pH, metMb has an iron-bound water molecule H bonded to the distal histidine; however, in the distal mutant His64Gln, the H bond is lost (Quillin et al., 1992). The CT1 band positions obtained for these two cases were 633 and 637 nm (Ikeda-Saito et al., 1992), corresponding to the H bonded and non-H bonded states, respectively, of the distal water molecule.

Inspection of the CT1 band positions for HRP-C* and its distal mutants (Table 1) enables a number of observations to be made on the H bonding interactions involving the sixth ligand of the hexacoordinate hemes. The three distal mutants H42L, R38G, and F41V are characterized by an increase in the population of the 6cHS species compared with that of HRP-C*. This is shown by the red-shifted Soret, the increased Soret extinction coefficient, and the decreased intensity of the shoulder at about 380 nm. However, the CT1 maximum is fairly different for the three mutants, being positioned at 633 and 635 nm for R38G and F41V, respectively, but remaining apparently unchanged compared to the parent enzyme for H42L (643 nm). Moreover, the RR core size marker bands indicate that the H42L mutant is dominated by a 6cHS$^{\#}$ heme, whereas the other two mutants have relatively more 6cHS heme. The wavelengths of the CT1 bands for the former two proteins indicate that the water molecule, which occupies the sixth coordinate position of the iron atom, is H bonded. An analogy with metMb suggests that the H bond is most probably with the N atom of the distal histidine. If one compares the CT1 wavelengths of the H42L mutant (643 nm) with that expected in the case when H bonding interactions with the iron bound water molecule are absent (∼637 nm, by analogy with the metMb mutant described above), it is apparent that the H42L CT1 band is significantly red-shifted. This indicates that the 6cHS$^{\#}$ heme form (the dominant heme state in the H42L mutant) is characterized by H bonding between the distal water molecule and the Arg38 residue, in which the water molecule acts as a H bond acceptor. Moreover, this analysis confirms that the HRP-C heme spin state assigned as 6cHS$^{\#}$ is in fact a hexacoordinate form; otherwise, its CT1 band would be red-shifted and the Soret band blue-shifted to values closely resembling those observed for the R38L variant, which has a dominant pentacoordinate heme state.

Effect of BHA. The absorption and RR spectra of wild-type HRP-C* and its distal mutants display a very variable response to the presence of BHA (Table 1). HRP-C* and the F41V mutant showed marked changes on binding BHA, the RR results being indicative of a mixture of two 6cHS hemes in the BHA complex (Smulevich et al., 1994b). This is the same behavior that has been found for H42L.

No changes were detected in the RR spectra in the presence of BHA for the variants R38K and F41W (Smulevich et al., 1994b), in agreement with the results of Smith et al. (1993), suggesting that the binding site of this donor had been changed in these two variants. However, a limited degree of spectral modification was induced by BHA in the RR spectra of mutants H42R, R38G, and R38L. Moreover, a variable amount of 5cHS$^{\#}$ heme remains in their BHA complexes. It follows that the relative populations of the heme spin states have not been drastically changed because BHA binds poorly to all these mutants.

The different effects observed for R38K compared to those for the R38G and R38L variants in the presence of BHA clearly must result from the different characteristics of the residues. The leucine and glycine residues are nonpolar and have relatively short side chains compared to the polar lysine residue. The RR results show that the R38K mutant is partially low-spin, indicating partial bonding of the lysine, hindering the binding of BHA. The R38G mutant remains essentially 6cHS, indicating that a water molecule is bound to the iron with and without BHA. A significant proportion of the R38L mutant remains 5cHS$^{\#}$ in the presence of BHA; and therefore, the distal cavity is relatively empty. The predominance of the hexacoordinate heme forms in the R38G mutant with and without BHA contrasts markedly with the pentacoordinate heme state displayed by the R38L variant with and without BHA. The R38L mutant is essentially characterized by a high-spin heme displaying anomalous RR frequencies, which in its water-ligated form (6cHS$^{\#}$) has been shown to be characterized by a H bond between the water molecule and Arg38. The R38G variant exists largely as the normal 6cHS heme state, characterized by H bonding between the distal water molecule and His42. Therefore,

one may speculate that the high population of the 5cHS$^{\#}$ state for R38L is due to the absence of a stabilizing H bond between the distal water molecule and Arg38. Consequently, it is suggested that H bonds with the distal residues are of some importance in retaining the water molecule in the cavity, although some influence due to a steric hindrance created by the leucine side chain which impedes binding of the water molecule to the heme iron is possible. It is apparent that BHA binds poorly to all the Arg38 mutants, demonstrating the importance of Arg38 in BHA binding.

The RR results for the H42R mutant are not helpful to our understanding of the role played by the distal histidine in BHA binding to HRP-C. The RR spectra of the mutant with and without BHA are dominated by 6cHS and 6cLS hemes, resulting from an iron-bound hydroxyl group (see below), which presumably blocks BHA binding. The distal cavity is too disrupted by the large polar arginine residue; replacement by the relatively small nonpolar leucine residue renders the H42L mutant more informative. The absorption and RR spectra indicate that BHA binds well to H42L, despite a higher dissociation constant for BHA compared to that for HRP-C*, indicating that His42 has a less important role in BHA binding than Arg38.

Consideration of the CT1 band positions of the BHA complexes (Table 1) allows one to assess the involvement of BHA and the distal histidine and arginine residues in H bonding interactions with the iron-bound water molecule when BHA is bound to the protein. As BHA is expected to act as a H bond acceptor at pH 7, H bonding interactions in which the distal water molecule acts as a H bond donor can potentially be with the distal histidine and/or BHA. Clearly, interactions with BHA or the histidine residue are indistinguishable. Only the enzymes which manifest significant spectral changes on addition of BHA, *i.e.* HRP-C*, H42L, R38L, and F41V, are discussed. It is clear from Table 1 that the BHA complexes of all four proteins are dominated by 6cHS and/or 6cHS$^{\#}$. In HRP−BHA, which has a dominant 6cHS$^{\#}$ heme state, the CT1 band at 639 nm is slightly red-shifted with respect to the case in which H bonds with the iron-bound water molecule are absent (CT1 at ∼637 nm), indicative of a weak H bond with Arg38. It is recalled that for the 6cHS$^{\#}$ heme state in the absence of BHA the CT1 band (at 643 nm) was more strongly red-shifted, suggesting that the H bond between the water molecule and the arginine residue is considerably weaker in the presence of BHA. This effect can be understood if the binding of BHA causes a displacement of the arginine residue. The CT1 band at 639 nm for both the HRP−BHA and H42L−BHA complexes (the latter having a dominant 6cHS heme state) suggests that the distal histidine is not directly involved in H bonding with the Fe-coordinated water molecule. In the R38L−BHA complex, the 6cHS heme (CT1 at ∼633 nm) plus the 5cHS$^{\#}$ heme (CT1 at ∼645 nm) together constitute the largest proportion of heme states, consistent with a resultant CT1 band at 638 nm. The F41V mutant binds BHA very well, giving a dominant 6cHS heme state consistent with a CT1 band at 635 nm and H bonding with His42 or BHA.

Analysis of data from different spectroscopic techniques, primarily NMR, has enabled a number of general indications to be made concerning the location of the aromatic donor molecule binding site. Aromatic hydrogen donor substrates (*e.g.* guaiacol, *p*-cresol) are proposed to bind to peripheral sites near the *δ-meso* and C18H3 heme edge, about 8−11 Å from the iron. Other substrates, exemplified by the commonly used active site probe BHA, are suggested to bind to a distal heme site (Veitch, 1995; Loew et al., 1995). There has been much speculation in the literature concerning the roles played by the distal arginine and histidine in BHA binding. Hydrogen-bonding interactions with either the distal arginine or histidine were considered important for BHA binding (Smulevich et al., 1994b; Smith et al., 1993; Veitch, 1993; La Mar et al., 1992); however, recent studies by Rodriguez-Lopez et al. (1996b) suggest that interactions with both distal residues are important for BHA binding. They propose a model, on the basis of determinations of the dissociation constant for BHA binding to R38L and H42L, in which both residues act in concert through a process resembling that proposed to occur during Compound I formation. Namely, there is an electrostatic interaction between the positive charge of the Arg38 and the negative charge of the oxygen on the BHA side chain concomitant with a H bond to the His42. It is evident from our results and the forgoing discussion that the Arg38 residue is of fundamental importance in BHA binding to HRP-C; however, while the distal histidine apparently acts in concert with Arg38, the extent of involvement of the distal histidine in BHA binding remains ill-defined, although it clearly performs a role secondary to that of Arg38.

Small Anion Binding and Implications for the Catalytic Mechanism. HRP-C* has a dissociation constant for fluoride of 5.7×10^{-4} M at pH 5 (Dunford & Alberty, 1967), but distal mutations have been found to markedly affect the binding of fluoride ions (data not shown). The R38L mutant exhibited the most pronounced effect, no adduct with F^- being formed even for a considerable excess of fluoride. A similar absence of adduct formation has been noted for OH^- ions at alkaline pH for all three Arg38 mutants (R38G, R38L, and R38K). The H42L mutant displayed a reduced capability to bind F^- compared to HRP-C*. For a considerable excess of F^-, the absorption spectrum was intermediate between that of the H42L variant alone and that observed for the HRP-C*−F^- adduct. These results are in general agreement with those seen for the binding of small ligands (*viz.* F^- and OH^-) to the corresponding distal mutants of CCP and CIP (F. Neri and G. Smulevich, unpublished results). The fact that the Arg → Leu distal variants do not form an adduct with F^- or OH^- for all three proteins implies that the distal arginine plays an important role in ligand stabilization. The distal histidine appears to be of secondary importance in ligand binding. The critical role of the arginine in H bonding stabilization of F^- and CN^- adducts of wild-type CCP has been clearly established by the crystal structure of these complexes (Edwards & Poulos, 1990). The importance of the distal histidine could not be so clearly assessed. It was proposed that the histidine acts as a H bond acceptor and therefore cannot H bond with fluoride in its basic F^- form, but it may possibly become protonated on ligand binding, presumably as a result of dissociation of the neutral form (HF) at the active site. A somewhat similar argument was suggested by Erman (1974). A CN^- binding study of HRP-C* distal mutants (Meunier et al., 1995) suggests similarities in the roles of the distal histidine and arginine residues of HRP-C* and CCP.

Wild-type HRP-C undergoes a transition to essentially a 6cLS heme at alkaline pH. Sitter et al. (1988) identified the

low-spin ν(Fe−OH) stretching mode at 503 cm^{-1} by ^{18}O and ^{54}Fe substitution. Subsequent RR measurements (Feis et al., 1994) showed that the iron-bound hydroxyl group is hydrogen bonded to a distal residue, the Arg38 residue being indicated as the most probable. Furthermore, the absence of an alkaline transition for the R38G, R38L, and R38K mutants demonstrates that the distal arginine is essential for the Fe−OH bond to form.

The presence of a mixture of high-spin and low-spin hemes in the H42L variant at alkaline pH prompts a description of the parent enzyme at pH 12 in which there is H bonding between the iron hydroxyl group and both the distal His42 and Arg38 residues. The hydroxyl group acts as a H bond donor to the histidine, as originally proposed by Sitter et al. (1988). However, there must also be a strong H bond between the hydroxyl group and the positively charged guanidinium group of Arg38; *i.e.* the hydroxyl group acts as a H bond acceptor in this case.

The binding of hydroxyl ions to the heme iron of the H42R mutant has been observed at both neutral and alkaline pH. The low-frequency RR spectra obtained in H_2O/D_2O at pH 7 and 12 reveal an isotope-sensitive mode at 501 cm^{-1} assigned as a ν(Fe−OH) high-spin stretching mode. The low-spin ν(Fe−OD) stretching mode of H42R is placed at 505 cm^{-1} in the low-frequency D_2O RR spectrum. (Figure 4). The observation of the low-spin band, which is expected to upshift on deuteration (Feis et al., 1994) rather than downshift as occurs for the high-spin band, supports the assignment of the band at 490 cm^{-1} in the H42R D_2O spectrum as being due to the high-spin heme. The failure to identify the low-spin ν(Fe−OH) mode in the H42L mutant is possibly due to a slightly lower proportion of low-spin heme in H42L, combined with the general difficulty of observing this band as a consequence of its expected low intensity (Feis et al., 1994) and proximity to the porphyrin band at 499 cm^{-1}.

The apparent formation of an iron−hydroxyl bond at pH 7 in the H42R mutant is suggested to result from a lowering of the pK_a of the second Arg residue (Arg42), from its intrinsic value of about 12 (Creighton, 1993), due to the presence of Arg38. The striking effect that the enzyme environment can have on the pK_a of an amino acid is demonstrated by acetoacetate decarboxylase (Abeles et al., 1992). The pK_a of a lysine residue in the active site of the enzyme was reduced to 6, from an intrinsic value of about 11. This decrease in pK_a is caused by electrostatic destabilization of the lysine amino group by adjacent positive charges, which favors dissociation of the proton.

If one accepts the premise that at pH 7 Arg42 is not protonated, the iron-bound water molecule can be a H bond donor with Arg42 while at the same time being a H bond acceptor with Arg38. If the H bond with Arg42 is stronger, the net result of such H bonding interactions is that the water molecule will assume a certain hydroxylate character. It is evident from this argument that the iron ligand in H42R has a less pronounced hydroxylate character than that of H42L at pH 12, which has an iron-bound OH^- group. The more protonated nature of the ligand in H42R is consistent with the 5 nm red shift of the high-spin charge transfer band of H42R at pH 7 compared to that of H42L at pH 12 (Smulevich et al., 1996).

A further difference between the H42L and H42R mutants is the 8 cm^{-1} upshift of the ν(Fe−OH) high-spin stretching frequency of H42R compared to that of H42L, which clearly implies that the force constant of the Fe−O bond is greater in H42R. A strengthening of the Fe−O bond in H42R is consistent with its increased proportion of 6cLS heme. It appears probable that both effects result from the establishment of H bonding with a second residue (Arg42) absent in H42L. However, the H bonding with Arg42 in H42R is not optimum as in wild-type HRP-C*, and consequently, only a slight return to the fully low-spin situation seen in HRP-C* is possible. The apparent invariance of the high-spin ν(Fe−OH) RR band (at 501 cm^{-1}) and charge transfer band (at 607 nm) in H42R at pH 12 compared to those at pH 7 strongly suggests that the geometrical arrangement and interactions proposed to exist at pH 7 are essentially unchanged at pH 12; *i.e.* a hydroxyl group, as such, appears not to bind at pH 12. The presence of a high-spin heme state, at pH 7 and 12, in H42R is somewhat unexpected on the basis of the forgoing considerations where all H bonds are assumed to be relatively strong. Nevertheless, some disruption of the distal cavity is perhaps to be expected due to the second large Arg residue which may introduce some flexibility in the positions of the Arg38 and Arg42 residues.

In light of the similarity between the alkaline transition mechanism of HRP-C, in which a concerted involvement of His42 and Arg38 is proposed, the effect on fluoride binding of mutating the His42 and Arg38 residues, and the fundamental features of the catalytic mechanism of CCP (Poulos & Kraut, 1980), there are strong indications that the catalytic mechanism of HRP-C and CCP are very similar. It has been proposed that, in the first step of the reaction cycle, the bound HOO^- group is stabilized by the positive charge of the guanidinium group of the distal arginine. At this stage, the bound HOO^- donates its proton to the unprotonated distal histidine. Therefore, ligand stabilization by the distal arginine is coupled to distal histidine protonation. The distal histidine acts as an acid−base catalyst by directing transfer of the peroxidase proton. The analogy between the catalytic reaction and the concerted mechanism of the alkaline transition, with the HOO^- group replaced by OH^-, is immediately apparent.

The key residues involved in the catalytic mechanism of CCP are highly conserved in HRP-C. Therefore, it is of keen interest to investigate the effects of mutating the distal histidine and arginine residues on the rate of Compound I formation in HRP-C. Such a study has recently been carried out (Rodriguez-Lopez et al., 1996a,b), and the results were compared with corresponding mutations in CCP (Erman et al., 1993; Vitello et al., 1993). It was found that the distal mutations Arg → Leu and Lys gave a larger decrease in peroxidase activity in HRP-C than in CCP. It was suggested that this perhaps indicates that the distal cavity of HRP-C resembles more closely that of the globins, which lack the distal arginine found in peroxidases, than does CCP. Furthermore, it suggests that Arg38 may have a more important function in HRP-C and that the detailed architecture of the distal cavity in HRP-C and CCP is different. The rate of Compound I formation for H42L was 5 orders of magnitude slower than that for wild-type HRP-C*. A very similar result was found for the analogous mutant of CCP, clearly demonstrating the significant role played by the distal histidine in the catalytic mechanism of both CCP and HRP-C.

The role of the distal histidine in the catalytic mechanism of HRP-C has also been recently investigated by determining the effects on the rate of Compound I formation of the mutations His42 → Ala and Val (Newmyer & Ortiz de Montellano, 1995). Both mutations compromised the catalytic process, giving a decrease of 6 orders of magnitude in the rate of Compound I formation. The conclusion that one draws from all these studies is that the evidence is considerably strengthened in favor of the direct involvement of both the distal histidine and arginine in the catalytic mechanism of HRP-C, in a manner similar to that originally proposed for CCP.

Ferrous Hemes. The ν(Fe−Im) stretching mode is sensitive to the strength of the strong H bond between the N_δ proton of the proximal imidazole and the proximal aspartate, which is present in all peroxidases. The frequency of this mode found in peroxidases is higher than in other hemoproteins as a direct result of the polar H bond between the conserved proximal histidine and aspartate residues. The degree of the shift depends on the strength of the H bond (Teraoka & Kitagawa, 1981; Smulevich et al., 1988a). The H42L, R38G, R38L, and R38K mutations cause a significant downshift in the frequency, with respect to that of wild-type protein (Table 3). The H42R and F41V mutations cause a very limited downshift of only 1 cm^{-1}. Therefore, one may infer that mutation of the distal arginine and replacement of the distal histidine by leucine weaken the H bond between the proximal histidine and aspartate residues. This presumably reflects a more neutral, less imidazolate character, of the axial ligand. A similar behavior has been found in CCP which exhibits two components of the ν(Fe−Im) stretching mode, resulting from two different H bond tautomers (Table 3). The H52L mutant of CCP, as the CCP R48L distal variant, displays a weakening of the H bond between the proximal histidine and aspartate residues. These effects have been considered to result from perturbations of the H bonding network, extending between the distal and proximal sides of the heme, due to the distal mutations. The polar side chain in the HRP-C H42R and CCP R48K variants appears able to maintain the H bonding interactions with the distal water molecules found in the wild-type enzymes. Consequently, they do not significantly perturb the H bonding network.

ACKNOWLEDGMENT

We are grateful to Prof. M. P. Marzocchi for stimulating discussions.

REFERENCES

Abeles, R. H., Frey, P. A., & Jencks, W. P. (1992) in *Biochemistry*, pp 105−106, Jones & Bartlett, London.

Asher, S. A., & Schuster, T. M. (1979) *Biochemistry 18*, 5377.

Asher, S. A., Adams, M. L., & Schuster, T. M. (1981) *Biochemistry 20*, 3339−3346.

Choi, S., Spiro, T. G., Langry, K. C., Smith, K. M., Budd, D. L., & La Mar, G. N. (1982) *J. Am. Chem. Soc. 104*, 4345−4351.

Creighton, T. E. (1993) in *Proteins: Structures and Molecular Properties*, Freeman & Co., New York.

Dasgupta, S., Rousseau, D. L., Anni, H., & Yonetani, T. (1989) *J. Biol. Chem. 264*, 654.

Dunford, H. B. (1991) in *Peroxidases in Chemistry and Biology* (Everse, J., Everse, K. E., & Grisham, M. B., Eds.) Vol. II, pp 1−24, CRC Press, Boca Raton, FL.

Dunford, H. B., & Alberty, R. A. (1967) *Biochemistry 6*, 447−451.

Dunford, H. B., & Stillman, J. S. (1976) *Coord. Chem. 19*, 187−251.

Edwards, S. L., & Poulos, T. L. (1990) *J. Biol. Chem. 265*, 2588−2595.

Erman, J. E. (1974) *Biochemistry 13*, 34−39.

Erman, J. E., Vitello, L. B., Miller, M. A., Shaw, A., Brown, K. A., & Kraut, J. (1993) *Biochemistry 32*, 9798−9806.

Evangelista-Kirkup, R., Grisanti, M., Poulos, T. L., & Spiro, T. G. (1985) *FEBS Lett. 190*, 221.

Feis, A., Marzocchi, M. P., Paoli, M., & Smulevich, G. (1994) *Biochemistry 33*, 4577−4583.

Finzel, B. C., Poulos, T. L., & Kraut, J. (1984) *J. Biol. Chem. 259*, 13027−13036.

George, P., Beetlestone, J., & Griffith, J. S. (1964) *Rev. Mod. Phys. 36*, 441.

Hashimoto, S., Teraoka, J., Inubishi, T., Yonetani, T., & Kitagawa, T. (1986) *J. Biol. Chem. 261*, 11110.

Ikeda-Saito, M., Hori, H., Andersson, L. A., Prince, R. C., Pickering, I. J., George, G. N., Sanders, C. R., Lutz, R. S., McKelvey, E. J., & Mattera, R. (1992) *J. Biol. Chem. 267*, 22843−22852.

La Mar, G. N., Hernandez, G., & de Ropp, J. S. (1992) *Biochemistry 31*, 9158−9168.

Loew, G. H., Du, P., & Smith, A. T. (1995) *Biochem. Soc. Trans. 23*, 250−256.

Meunier, B., Rodriguez-Lopez, J. N., Smith, A. T., Thorneley, R. N. F., & Rich, P. R. (1995) *Biochemistry 34*, 14687−14692.

Newmyer, S. L., & Ortiz de Montellano, P. R. (1995) *J. Biol. Chem. 270*, 19430−19438.

Poulos, T. L., & Kraut, J. (1980) *J. Biol. Chem. 255*, 8199.

Quillin, M. L., Brantley, R. E., Jr., Johnson, K. A., Olson, J. S., & Phillips, G. N., Jr. (1992) *Biophys. J. 61*, A446.

Rakshit, G., & Spiro, T. G. (1974) *Biochemistry 13*, 5317.

Rodriguez-Lopez, J. N., Smith, A. T., & Thorneley, R. N. F. (1996a) *J. Biol. Chem. 271*, 4023−4030.

Rodriguez-Lopez, J. N., Smith, A. T., & Thorneley, R. N. F. (1996b) *J. Biol. Inorg. Chem. 1*, 136−142.

Sanders, S. A., Bray, R. C., & Smith, A. T. (1994) *Eur. J. Biochem. 224*, 1029−1037.

Schuller, D. J., Ban, N., van Huystee, R. B., McPherson, A., & Poulos, T. L. (1996) *Structure 4*, 311−321.

Sievers, G., Osterlund, K., & Ellfolk, N. (1979) *Biochim. Biophys. Acta 581*, 1.

Sitter, A. J., Shifflett, J. R., & Terner, J. (1988) *J. Biol. Chem. 263*, 13032−13038.

Smith, A. T., Santama, N., Dacey, S., Edwards, M., Bray, R. C., Thorneley, R. N. F., & Burke, J. F. (1990) *J. Biol. Chem. 265*, 1335.

Smith, A. T., Sanders, S. A., Thorneley, R. N. F., Burke, J. F., & Bray, R. C. (1992) *Eur. J. Biochem. 207*, 507−519.

Smith, A. T., Sanders, S. A., Sampson, C., Bray, R. C., Burke, J. F., & Thorneley, R. N. F. (1993) in *Plant Peroxidases: Biochemistry and Physiology, III International Symposium Proceedings* (Welinder, K. G., Rasmussen, S. K., Penel, C., & Greppin, H., Eds.) pp 159−168, University of Geneva, Geneva, Switzerland.

Smith, A. T., Du, P., & Loew, G. H. (1994) in *Nuclear Magnetic Resonance of Paramagnetic Molecules* (La Mar, G. N., Ed.) pp 75−93, Kluwer Academic Publishers, Dordrecht, The Netherlands.

Smulevich, G. (1993) in *Biomolecular Spectroscopy, Part A* (Clark, R. J. H., & Hester, R. E., Eds.) pp 163−193, Wiley & Sons, New York.

Smulevich, G., Mauro, J. M., Fishel, L. F., English, A. M., Kraut, J., & Spiro, T. G. (1988a) *Biochemistry 27*, 5477−5485.

Smulevich, G., Mauro, J. M., Fishel, L. F., English, A. M., Kraut, J., & Spiro, T. G. (1988b) *Biochemistry 27*, 5486−5492.

Smulevich, G., Mantini, A. R., English, A. M., & Mauro, J. M. (1989a) *Biochemistry 28*, 5058−5064.

Smulevich, G., Miller, M. A., Gosztola, D., & Spiro, T. G. (1989b) *Biochemistry 28*, 9905−9908.

Smulevich, G., Wang, Y., Edwards, S. L., Poulos, T. L., English, A. M., & Spiro, T. G. (1990a) *Biochemistry 29*, 2586−2592.

Smulevich, G., Wang, Y., Mauro, J. M., Wang, J., Fishel, L. A., Kraut, J., & Spiro, T. G. (1990b) *Biochemistry 29*, 7174−7180.

Smulevich, G., English, A. M., Mantini, A. R., & Marzocchi, M. P. (1991a) *Biochemistry 30*, 772−779.

Smulevich, G., Miller, M. A., Kraut, J., & Spiro, T. G. (1991b) *Biochemistry 30*, 9546−9558.
Smulevich, G., Feis, A., Focardi, C., Tams, J., & Welinder, K. G. (1994a) *Biochemistry 33*, 15425−15432.
Smulevich, G., Paoli, M., Burke, J. F., Sanders, S. A., Thorneley, R. N. F., & Smith, A. T. (1994b) *Biochemistry 33*, 7398−7407.
Smulevich, G., Neri, F., Marzocchi, M. P., & Welinder, K. G. (1996) *Biochemistry 35*, 10576−10585.
Smulevich, G., Paoli, M., De Sanctis, G., Mantini, A. R., Ascoli, F., & Coletta, M. (1997) *Biochemistry 36*, 640−649.
Teraoka, J., & Kitagawa, T. (1981) *J. Biol. Chem. 256*, 3969−3977.
Terner, J., & Reed, D. E. (1984) *Biochim. Biophys. Acta 789*, 80.
Veitch, N. C. (1993) in *Plant Peroxidases: Biochemistry and Physiology, III International Symposium Proceedings* (Welinder, K. G., Rasmussen, S. K., Penel, C., & Greppin, H., Eds.) pp 57−64, University of Geneva, Geneva, Switzerland.
Veitch, N. C. (1995) *Biochem. Soc. Trans. 23*, 232−240.
Veitch, N. C., Williams, R. J. P., Bray, R. C., Burke, J. F., Sanders, S. A., Thorneley, R. N. F., & Smith, A. T. (1992) *Eur. J. Biochem. 207*, 521−531.
Vitello, L. B., Erman, J. E., Miller, M. A., Mauro, J. M., & Kraut, J. (1992) *Biochemistry 31*, 11524−11535.
Vitello, L. B., Erman, J. E., Miller, M. A., Wang, J., & Kraut, J. (1993) *Biochemistry 32*, 9807−9818.
Welinder, K. G. (1992) *Curr. Opin. Struct. Biol. 2*, 388−393.

BI962502O